Proceedings of the 4th International Conference on Biological Engineering and Medical Science
DOI: 10.54254/2753-8818/59/20241348

# Self-Assembling Chimeric Polypeptides as Drug-Carrying Nanoparticles for Anti-Cancer Chemotherapy

**Andrew Huang**

The Webb Schools of California, Claremont, CA 91711, US

andrewhuang20080616@gmail.com

**Abstract.** Chemotherapy is often limited by unfavorable pharmacokinetics and pharmacodynamics that result in dose-limiting cytotoxicity. Therefore, self-assembling nanoparticles have been of particular interest to address these limitations by altering the physicochemical properties of payloads. Amphiphilic chimeric polypeptides (CPs) capable of versatile payload conjugation and spontaneous self-assembly into monodisperse micelles were designed, recombinantly synthesized, and characterized in this study. Doxorubicin (Dox) was also conjugated onto CPs to determine the effectiveness of pH-mediated release and the effects of payload conjugation on CP morphology. The designed CP consisted of a hydrophilic elastin-like polypeptide that enabled non-chromatographic polypeptide purification, an aspartic acid linker, a short Cys-rich segment for drug conjugation, and a hydrophobic domain that promoted the spontaneous formation of CP nanoparticles. Additionally, bio-orthogonal conjugation of chemotherapeutics onto CPs through short acid-labile chemical linkers enabled controlled pH-mediated release of conjugated chemotherapeutics and enhanced self-assembly. Results indicated that CP and Dox-CP nanoparticles had critical aggregation concentrations of 3.24 and 0.58 μM and hydrodynamic radii of 57.09 and 72.86 nm, respectively. Dox-CP also released 76.8% of conjugated chemotherapeutics after 24 hours in late endosome pH and was effective against triple-negative breast cancer cells. These favorable characteristics and the independent self-assembly of the designed CP will enable targeted chemotherapeutic delivery regardless of payload hydrophobicity.

**Keywords:** elastin-like polypeptides, drug delivery, chimeric polypeptides, nanoparticles

## 1. Introduction

Encapsulation of clinically approved drugs into nanoscale (10-200 nm diameter), versatile packages are of particular interest for chemotherapy as the enhanced permeability and retention (EPR) effect present within solid tumors through angiogenesis and abnormalities in lymphatic vasculature enables accumulation of nanoparticles of that size within endothelial gaps [1,2]. However, effective and versatile drug loaded nanoparticles must: i) be readily synthesized in high purity and yield; ii) exhibit exceptional pharmacokinetics; iii) release encapsulated drugs under controllable and tunable mechanisms; iv) improve physiological conditions without immunogenic response; and v) enable conjugation of multiple drugs for synergy [3-7]. Although numerous similar delivery systems have been reported in past decades, few satisfy all above criteria that enable clinical application.

DOI: 10.54254/2753-8818/59/20241348

Motivated by the aforementioned challenges, I designed a chimeric polypeptide (CP) delivery system that can self-assemble into micelles in aqueous solutions and enable bio-orthogonal conjugation of multiple chemotherapeutics. This CP was recombinantly synthesized to ensure sequence precision at the amino acid level and purified using inverse transition cycling (ITC). The CP was designed to possess a MW of 65.7 kDa and was composed of three main segments: i) a 160-repeat elastin-like polypeptide (ELP) with alanine guest residues; ii) a cysteine-rich drug conjugation domain; and iii) a hydrophobic self-assembly domain (Fig. 1A). ELPs are a class of artificial human tropoelastin derived polymers composed of repeating pentapeptides VPGXG, with X representing any amino acid residue except proline [8]. ELPs exhibit lower critical solution temperature (LCST), where they undergo reversible entropy-driven phase transition above a transition temperature ($T_t$) and become insoluble in aqueous solutions as the number of intrapeptide hydrogen bonds within ELPs increases and spontaneous water-ELP interactions decrease [9,10]. $T_t$ can be manipulated through ELP guest residues and the number of ELP pentapeptide repeats [8,11-13]. Hence, ELPs can possess specific $T_t$ through recombinant synthesis in *Escherichia coli*, where the molecular weight, guest residue, and number of pentapeptide repeats are strictly controlled [14]. ELP-containing polypeptides can also be purified in high yields through ITC, which utilizes ELP phase transition and centrifugation to produce high-purity material [15]. The ELP component of this CP was designed to be hydrophilic to provide sufficient amphiphilicity for CP self-assembly. It was also designed to have a MW of ~61.05 kDa and a $T_t$ > 37 °C to ensure solubility at body temperature and low-cost CP purification. The drug attachment domain $(CGG)_8$ was fused to the C terminus of the ELP using a $D_8$ linker to provide cysteine residues separated by di-glycine spacers to minimize steric hindrance. The CP also had a hydrophobic domain $(WG)_8$ attached to the C terminus of $(CGG)_8$ to provide sufficient amphiphilicity for spontaneous CP self-assembly into micelles in aqueous environments (Fig. 1B) [4]. This nanoparticle delivery system will enable targeted delivery of various chemotherapeutics into cancerous cells through pH-mediated release, which will improve systemic drug distribution and kinetics.

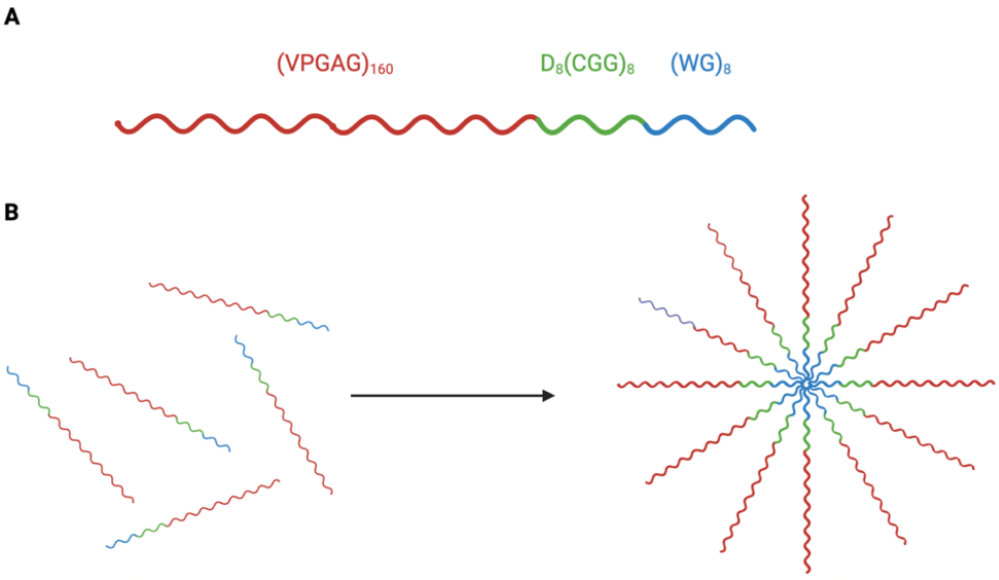


**Figure 1.** Structure and self-assemblage of CP. (A) Integral structures within the CP, composed of an ELP, drug attachment domain, and hydrophobic domain. (B) Self-assembly of multiple CPs into micelle-like nanoparticles under $T_t$ (made using BioRender.com).

Doxorubicin (Dox) was conjugated onto the CP to evaluate CP effectiveness in encapsulating chemotherapeutics. Dox is effective against a variety of cancers but also possesses dose-limiting cytotoxicity and cardiotoxicity [16]. Thus, Dox is a suitable candidate for CP encapsulation because CPs can limit Dox cytotoxicity to tumors while improving pharmacokinetics. Additionally, Dox conjugation

DOI: 10.54254/2753-8818/59/20241348

onto CPs through an acid-labile N-ε-maleimidocaproic acid hydrazide (EMCH) linker would enable pH-mediated release of Dox at late endosome pH through cleavage of the EMCH-Dox hydrazone bond [6]. CP and Dox-CP conjugates were characterized through cryogenic transmission electron microcopy (Cryo-TEM), dynamic light scattering (DLS), temperature-based spectrophotometry, and pyrene assay to determine CP nanoparticle morphology and the influence of Dox conjugation on CP characteristics. Dox-CP release kinetics were also determined through a pH-mediated release assay while Dox-CP cytotoxicity and effectiveness were determined through a cell-viability assay with MDA-MB-231 triple negative breast cancer cells.

## 2. Materials and Methods

### *2.1. Recombination vector construction and transformation*

The oligonucleotides encoding the CP were provided by Integrated DNA Technologies Inc (Coralville, IA). pET-28a(+) plasmids were purchased from Novagen Inc (Madison, WI). DNA mini-prep and gel purification kits were purchased from Qiagen Inc (Germantown, MD). Chemically competent *Escherichia coli* BL21-DE3 cells, restriction enzymes, and quick ligase were purchased from New England Biolabs (Ipswich, MA).

pET-28a(+) vector plasmids were digested by 2 U of HindIII for 16 hours at 37 °C. Upon digesting plasmids, HindIII was removed through gel purification. The linearized vectors were then dephosphorylated with 1 U CIP for 1 hour at 37 °C to reduce self-recirculation before being eluted in 30 μL of distilled DI water. Concatemers were ligated through incubation of 10 pmol of annealed dsDNA with 0.1 pmol linearized vector in 400 U T4 ligase buffer at 20 °C for 1 hour. Product was transformed into BL21-DE3 competent *E. coli*, which were allowed to recover at 37 °C in Luria broth and then plated on TBdry plates supplemented with 45 μg/mL kanamycin solution for antibiotic selection where positive transformants were extracted for cultivation.

### *2.2. Cultivation and purification of CP*

Recombinant *E. coli* were cultured in 250 mL flasks with 50 mL of 2x Yeast Extract Tryptone medium induced with 1 mM isopropyl-beta-β-thiogalactopyranoside (IPTG; Thermo Fisher Scientific, Waltham, MA) solution and 45 μg/mL kanamycin. After 1 day of culturing at 37 °C shaking, cultivated *E. coli* were distributed among 4 L flasks and cultured with 1 L of identical medium for another 24 hours under identical conditions to produce 12 1 L cultures. *E. coli* colonies were then collected with centrifugation at 3400 rpm for 15 minutes and lysed with sonication upon being resuspended in PBS. The nucleic acids in cell lysate were removed with a 10% PEI buffer, and the remaining supernatant was purified with three rounds of ITC [15]. In each cycle, lysate with 3.5 M NaCl solution was heated beyond $T_t$ to 55 °C, supernatant was removed, and the remaining solution was cooled below $T_t$ (4 °C) after addition of 30 mL 25 mM Tris(2-carboxyethyl)phosphine hydrochloride (TCEP; Sigma-Aldrich, St. Louis, MA) solution. Remaining pellets were removed before the process was repeated. Dialysis of solution against a dialysis membrane (MWCO=3 kDa) in Milli-Q water for 36 hours was then performed to remove any remaining impurities. Purification was verified through SDS-polyacrylamide gel electrophoresis.

### *2.3. Gel electrophoresis*

Upon completion of aforementioned purification, substantial amounts of protein samples from each purification were collected. 10 μL of each protein sample was aliquoted into separate Eppendorf tubes with 30 μL of 4x Laemmli loading buffer (Thermo Fisher Scientific; Waltham, MA) supplemented with 10% β-mercaptoethanol (Sigma-Aldrich; St. Louis, MA). After 12 minutes of incubation at 95 °C, tubes were centrifuged for one minute. A Mini-PROTEAN® TGX™ gel (Bio-Rad; Hercules, CA) was then prepared and placed in the gel box with tris-glycine-SDS running buffer (Sigma-Aldrich; St. Louis, MA). 6 μL of Kaleidoscope protein ladder (Bio-Rad; Hercules, CA) was added to the first lane of the gel and 12 μL of each protein sample was loaded into corresponding wells of the gel. The gel was run at 200 V for 30 minutes before the gel was removed, microwaved for 1 minute with DI water, stained with 20

DOI: 10.54254/2753-8818/59/20241348

mL of SimplyBlue™ solution (Thermo Fisher Scientific; Waltham, MA), and microwaved for 1 minute. Stain was then removed and the gel was washed with DI water before being imaged.

### *2.4. Conjugation of Dox onto CP*

In separate dry glass tubes, ~82 mg of EMCH (339.27 g $mol^{-1}$; Sigma-Aldrich, St. Louis, MA) and ~176 mg of Dox (580 g $mol^{-1}$) was prepared for 400 mg of CP so that the molar ratio of Dox to EMCH=1.25:1. Dox was dissolved in ~56 mL of anhydrous methanol supplemented with 70 μL of optically clear trifluoroacetic acid (TFA; Sigma Aldrich, St. Louis, MA). The solution was then transferred to a 250 mL bottom round flask where EMCH dissolved in ~14.4 mL of anhydrous methanol was immediately added to the Dox solution while stirring. Meanwhile, 400 mg of lyophilized CP was dissolved at a molar ratio of EMCH to thiol=5:1 in deoxylation buffer (0.1 M $Na_3PO_4$, 1 mM EDTA, pH 7.2) supplemented with 0.8 mL of 50 mM TCEP. Both solutions were stirred at room temperature overnight. After overnight reaction, methanol was separated from EMCH-Dox using rotary evaporation (water bath ~40 °C) and EMCH-Dox was resuspended in 20 mL of anhydrous methanol. CP solution was supplemented with 0.5 mL of 50 mM TCEP before being slowly added to the EMCH-Dox solution. The solution was stirred overnight at room temperature in the dark. Dox-CP solution was then centrifuged at 2000 rpm against a dialysis membrane (MWCO=3 kDa) to remove excess Dox and TCEP.

### *2.5. Cryogenic transmission electron microscopy*

10 μL of 25 μM CP and Dox-CP solutions were frozen and imaged using Cryo-TEM with a copper grid.

### *2.6. Dynamic light scattering*

Hydrodynamic radii of CP and Dox-CP were determined though DLS with a Zetasizer Nano S where nanoparticle diffusion coefficients determined from 1 mL of 25 μM CP and Dox-CP solutions in DI water at 25 °C were inserted into the Stokes-Einstein equation to determine hydrodynamic radius. Dox-CP and CP hydrodynamic radii were then characterized and distributed using percent by class.

### *2.7. Pyrene assay*

The CAC of CP and Dox-CP conjugates were estimated by fluorescence spectroscopy using pyrene as a fluorescent probe for local hydrophobicity. 20 mM of a pyrene stock solution was first prepared in ethanol and sonicated for 10 min at room temperature. Pyrene was then diluted to 1 mM using PBS. 100 μL of Dox-CP conjugates and CPs were dissolved in 1 mL of diluted pyrene solutions at 25 °C at concentrations of 0.001, 0.01, 0.05, 0.1, 0.5, 1, 5, 10, 25, 50, and 100 μM. Samples were then placed in an Agilent Cary 5000 UMA spectrophotometer for measurement where the fluorescence spectrum of each concentration was measured for Dox-CP and CP to calculate their intensity peak 1:3 ratios. The intensity ratios for each nanoparticle were separated into two groups by correlation, where the intersection point of linear regression lines from the two groups was used to determine CAC.

### *2.8. Transition temperature*

To determine $T_t$, 1 mL of 25 μM CP and Dox-CP solutions in DI water were placed within an Agilent Cary 300 UV-Vis spectrophotometer. The optical density at 350 nm was measured as a function of temperature where temperature increases at a rate of 1 °C/min.

### *2.9. Release kinetics*

2 μL of 1 mM Dox-CP solution was dissolved in pH 4.7 and 7.4 buffer made from PBS supplemented with hydrochloric acid. The dissolved CPs were kept in Slide-A-Lyzer™ MINI Dialysis Devices (MWCO=3.5 kDa; Thermo Fisher Scientific, Waltham, MA) at 37 °C to measure release. The released solution was measured at various time points over 24 hours for absorbance at 496 nm using an Agilent Cary 300 UV-Vis spectrophotometer. The absorbance of dialyzed Dox was compared to the absorbance of total conjugated Dox to determine percent released.

DOI: 10.54254/2753-8818/59/20241348

### *2.10. Cytotoxicity assay*

Triple-negative breast cancer cells MDA-MB-231 were purchased from the American Type Cell Collection (Manassas, VA) and thawed according to vendor instructions. Cells were cultured in 89% DMEM, 10% Fetal Bovine Serum, and 1% Penicillin-Streptomycin medium and incubated at 37 °C and pH 7.0. Cells were counted using a cell counter and subcultured at 70-80% cell confluency using 0.25% EDTA-trypsin until >96000 cells were obtained. Upon obtaining sufficient cells, 1000 cells were seeded per well on a 96-well plate and cultured overnight for 24 hours for cell adhesion. Culture medium was then replaced with drug-filled medium containing various concentrations of Dox and Dox-CP and cultured for 48 hours before medium was removed and replaced with CellTiter 96 AQueous™ (Promega; Madison, WI). Cells were cultured for an additional 2 hours and analyzed for cell viability using plate absorbance readings at 490 nm.

## 3. Results

### *3.1. Recombination and purification*

The sequence coding for the CP was expressed in *E. coli* cells through recombination on pET-28a(+) plasmids. After harvesting the cell lysate, the CP was purified through ITC. ITC exploits the phase transition nature of ELPs present within the CP and involves constant temperature variation between $T_t$ through hot and cold spins to isolate the CP (Fig. 2A) [15]. During the hot spin, cell lysate was buffered with kosmotropic salt to reduce the solubility of hydrophobes and enhance ELP phase transition before being heated > $T_t$ for the hot spin, where soluble impurities in supernatant were removed upon centrifugation as CP aggregates and form pellets within the solution. The remaining solution was then cooled to 4 °C (below $T_t$) for the cold spin where the responsive CP would spontaneously dissolve back into the solution while impurities remained insoluble. Pellets composed of insoluble impurities were then removed from the solution after centrifugation. After three rounds of ITC, the CP was successfully purified as evidenced by SDS-polyacrylamide gel electrophoresis. Sample supernatant extracted after each hot and cold spin was also used to verify purification as supernatant extracted from cold spins indicated gradual CP enrichment (Fig. 2B).

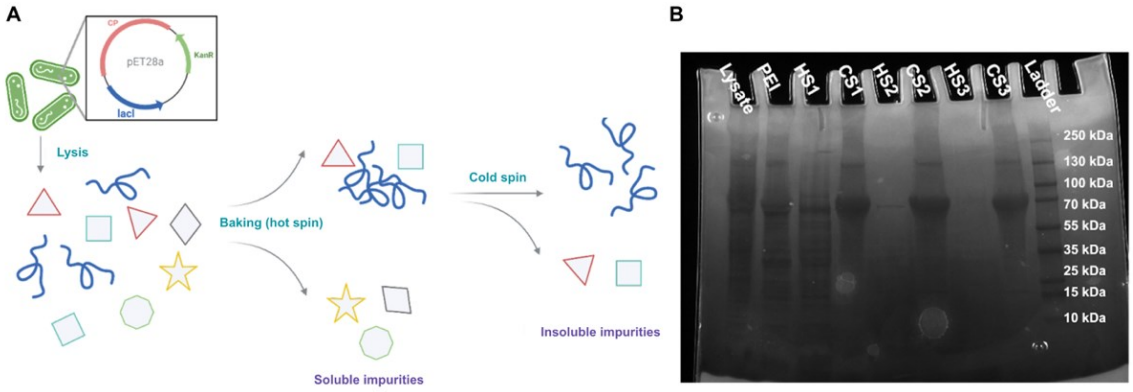


**Figure 2.** Synthesis and purification of CP. (A) CP was expressed in pET-28a(+) plasmid in E. coli to ensure recombinant biosynthesis and purification through ITC (made using BioRender.com). (B) SDS-polyacrylamide electrophoresis verification of successful CP purification after three ITC rotations.

### *3.2. Conjugation of Dox onto CPs*

Dox was conjugated onto the CPs through two reactions. Dox first reacted with EMCH in trifluoroacetic acid and anhydrous methanol to establish an acid-labile hydrazone bond that will enable pH-triggered intracellular release of Dox from CPs within late endosomes (Fig. 3A). The terminal maleimide of EMCH-Dox was then used as a conjugation site for subsequent covalent attachment onto CP cysteine residues (Fig. 3B). UV-Vis spectroscopy indicated that purified CP had a mean 3.7 drug conjugates from 8 conjugation sites per CP.

DOI: 10.54254/2753-8818/59/20241348

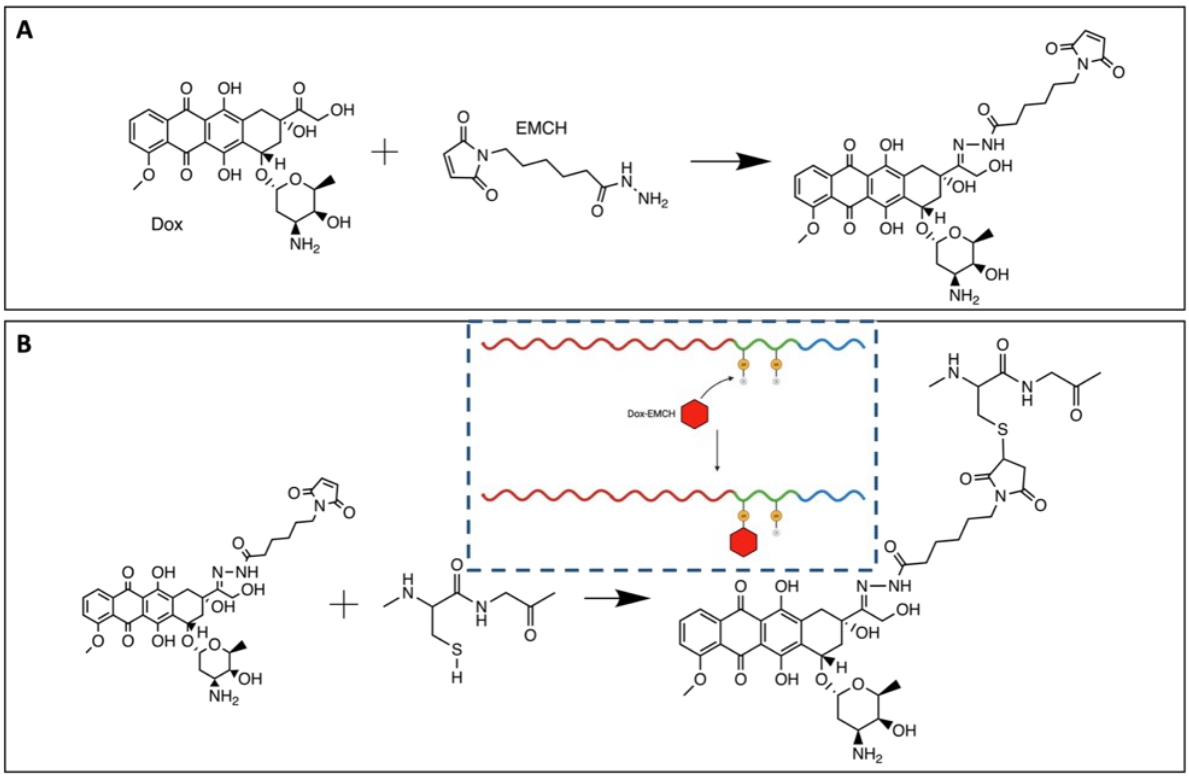


**Figure 3.** Conjugation of Dox onto CP. (A) Dox is conjugated onto the amino group of EMCH and forms a hydrazone bond. (B) A maleimide bond is formed between the maleimide in EMCH and thiol in the cysteine residue of the CP (cartoon representation made using BioRender.com).

### *3.3. Characterization of CP and Dox-CP*

To confirm spontaneous self-assembly of the amphiphilic CPs and determine the influence of Dox conjugation, I characterized the hydrodynamic size, morphology, and critical aggregation concentration (CAC) of CP nanoparticles. Results from DLS, Cryo-TEM, and pyrene assays confirmed that CP and Dox-CP conjugates self-assembled into micelle-like nanoparticles (Fig. 4). CPs and Dox-CPs that underwent Cryo-TEM were observed to be cylindrical while DLS indicated excellent monodispersity within the nanoparticles (Fig. 4B) and thus homogenous and size-dependent behavior. CP and Dox-CP also had mean hydrodynamic radii of 57.09 and 72.86 nm respectively and were determined to possess a $T_t$ of ~48 °C regardless of Dox conjugation (Fig. 4C). I then investigated whether Dox attachment would influence CP self-assembly because Dox would provide extra hydrophobicity to the CP. Dox-CP nanoparticles were observed in a pyrene assay to possess a CAC of 0.58 μM (Fig. 4E), suggesting lower necessary concentrations for self-assembly and prolonged circulation in vivo compared to regular CP nanoparticles that had a CAC of 3.24 μM (Fig. 4D).

DOI: 10.54254/2753-8818/59/20241348

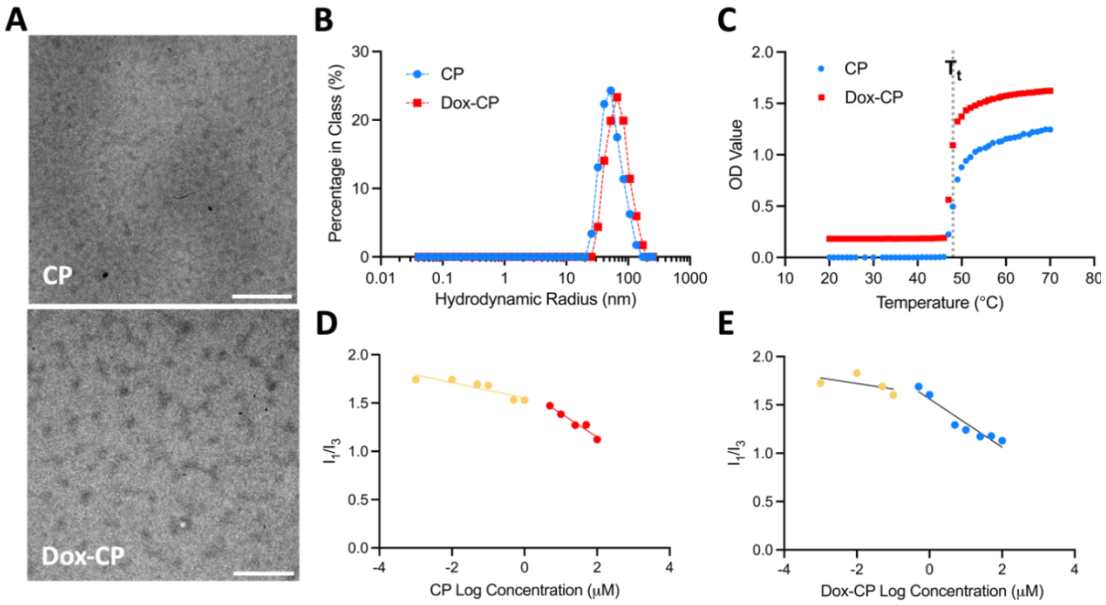


**Figure 4.** Characterization of CP and Dox-CP. (A) Cryo-TEM of CP (top) and Dox-CP (bottom) micelle structures (scale bar: 100 nm). (B) Hydrodynamic radii of CP and Dox-CP micelle structures determined through DLS. (C) $T_t$ of Dox-CP and CP. (D) CP CAC determined through a pyrene assay. (E) Dox-CP CAC determined through a pyrene assay.

### *3.4. Release kinetics and cytotoxicity assay*

The Dox-CP conjugates were designed to be pH sensitive through EMCH-Dox hydrazone bonds because micelles will be trafficked into endosomes upon cellular uptake, where endosome maturation and acidification would break down the EMCH-Dox hydrazone bonds and release active Dox. To quantify the pH-mediated release of Dox, I suspended Dox-CP in PBS buffered with HCl at pH 4.7 and 7.4 for 24 hours to evaluate the effectiveness of pH-mediated release within late endosomes and normal physiological conditions, respectively. Dox release was monitored through UV-Vis spectroscopy at 496 nm. At pH 7.4, Dox-CP hydrazone bonds were relatively stable, releasing only 16.22% of total conjugated drug after 24 hours. Contrastingly, Dox-CP released 76.8% of total conjugated drugs at pH 4.7, which confirms the stability of Dox-CP covalent bonds at physiological pH and the substantial release of Dox in pH relevant to endo-lysosomal trafficking. Overall, these kinetics will reduce undesired systemic toxicity and promote intratumoral drug release. Then, to validate Dox-CP cytotoxicity against cancer cells, MDA-MB-231 triple negative breast cancer cells were exposed to Dox-CP and free Dox to determine cytotoxicity after 48 hours. Free-Dox had an IC-50 of 0.19 μM while Dox-CP required 4.38 μM due to additional drug release kinetics hindering drug effectiveness.

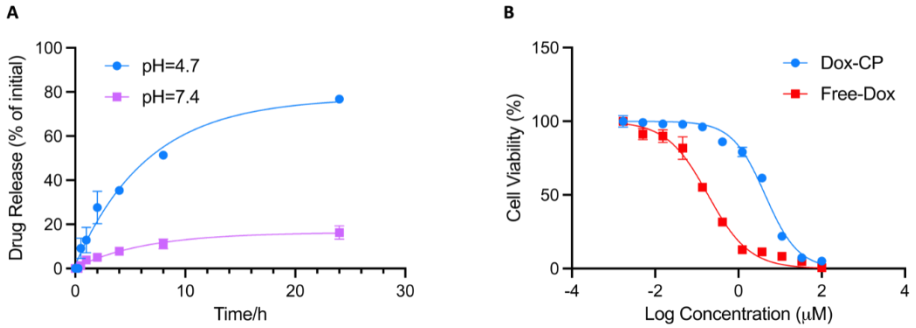


**Figure 5.** Release kinetics and cell viability. (A) pH triggered release of Dox over 24 hours. (B) Viability of MDA-MB-231 cells exposed to various Free-Dox and Dox-CP concentrations after 48 hours.

DOI: 10.54254/2753-8818/59/20241348

## 4. Discussion

The CPs described herein were versatile nanoparticles that could be efficiently synthesized and purified through low-cost simple processing of recombinant *E. coli*. Sufficient drug release in cell viability and release kinetics assays demonstrated CP control over release kinetics and CP effectiveness in late endosomal or lysosome environments where hydrazone bonds are cleaved to release chemotherapeutics through degradation of the acid-labile linker. Cryo-TEM and hydrodynamic radii also indicated favorable nanoparticle sizes in aqueous environments (between 100-200 nm) that fit within gaps created by the EPR effect. Furthermore, low CAC and high $T_t$ indicated low necessary concentration for spontaneous assemblage and ELP solubility at body temperature. Overall, the synthesized CPs displayed multiple favorable characteristics as drug-carrying nanoparticles.

The closest analog to the current design is a two-block CP designed by Mackay *et al*. [3] able to form micelles, but their self-assembly relies heavily on attached hydrophobic agents and hindered their usage for hydrophilic payloads. As a particular improvement, the designed CPs possessed greater versatility as drug-carrying nanoparticles. The self-assembly domain $(WG)_8$ enabled independent self-assembly of CPs into nanoparticles, bypassing the requirement of hydrophobic attachments for micelle formation. The drug conjugation domain also consisted of multiple nucleophilic residues, which enabled simultaneous attachment of multiple drugs for synergistic chemotherapeutic combinations. Hence, this CP will allow intracellular delivery of various chemotherapeutic combinations regardless of hydrophobicity. Moreover, concentrated drug conjugation domains will enhance amphiphilicity as therapeutic agents accumulate and contribute to the self-assembly of CP nanoparticles. The CAC of the designed CP was significantly lower compared to the design by Mackay *et al*. because the hydrophobic domain offers extra hydrophobicity for self-assembly, indicating self-assembly of functional nanoparticles at lower concentrations and potentially prolonged circulation in vivo. The designed CP also displayed favorable release of Dox under acidic pH, enabling efficient intracellular release of Dox in the late endosome. The designed CP has exhibited improved versatility and effectiveness compared to previous designs, but further optimization may be necessary. Compared to Mackay *et al*., lower CP yields were obtained from recombinant synthesis. The lower yield could be due to high GC content of the sequence, the hydrophobicity of the CP interfering with ribosomal processes, and a lack of yield-enhancing leader peptides (SKGPG). The designed CP also possessed lower drug conjugation ratios and formed larger nanoparticles possibly because of steric hindrance generated by the self-assembly domain and intrapeptide disulfide cysteine bonds. Overall, despite shortcomings in CP yield and conjugation, the designed CPs are versatile nanoparticles capable of independent self-assembly that display potential in delivering synergistic chemotherapeutic combinations.

In future study, several issues need to be addressed before clinical application. For instance, the stability of Dox-CP nanoparticles in plasma must be determined. Even though the acid-labile linker was proven to be stable in physiological pH, serum proteins will likely interact with the nanoparticles and generate unknown effects. Dox-CP pharmacokinetics and effectiveness in vivo also need to be evaluated to determine ideal therapeutic concentrations and potential immunogenic response. Moreover, given the independent self-assembly of the designed CP, further application via conjugation of synergizing chemotherapeutic pairs may be conducted to determine conjugate effects on CP self-assembly and release kinetics. Further experimentation with environmentally reliant linkers for drug conjugation must also be conducted to enhance drug release kinetics. Individual drugs likely require unique linkers to maximize release effectiveness, and hence, optimization with chemical linkers will be necessary to maximize CP effectiveness in delivering multiple chemotherapeutic agents. However, while further experimentation is necessary before clinical application, the designed CPs have demonstrated favorable characteristics and great potential as versatile drug-carrying nanoparticles.

The CPs described in this study possessed favorable characteristics and were effective as drug-carrying nanoparticles. The designed CPs were effective in eliminating triple-negative breast cancer cells and capable of pH-mediated payload release, with their small size and hydrodynamic radii also indicating favorable morphology as CP nanoparticles possessed dimensions capable of fitting within the 200 nm endothelial gaps created by the EPR effect. Moreover, independent CP self-assembly into

nanoparticles demonstrated the potential of CPs as versatile drug-carrying nanoparticles capable of delivering various chemotherapeutics regardless of hydrophobicity. Overall, the designed CPs have displayed favorable characteristics as drug-carrying nanoparticles and potential for delivering various chemotherapeutic agents.

## References

[1] Liu, W. *et al.* Tumor accumulation, degradation and pharmacokinetics of elastin-like polypeptides in nude mice. *J. Control. Release.* 116, 170–178 (2006).

[2] Wu, J. The enhanced permeability and retention (Epr) effect: The significance of the concept and methods to enhance its application. *J. Pers. Med.* 11, (2021).

[3] Andrew MacKay, J. *et al.* Self-assembling chimeric polypeptide-doxorubicin conjugate nanoparticles that abolish tumours after a single injection. *Nat. Mater.* 8, 993–999 (2009).

[4] Bhattacharyya, J. *et al.* Encapsulating a Hydrophilic Chemotherapeutic into Rod-Like Nanoparticles of a Genetically Encoded Asymmetric Triblock Polypeptide Improves Its Efficacy. *Adv. Funct. Mater.* 27, (2017).

[5] Chilkoti, A., Dreher, M. R. & Meyer, D. E. Design of Thermally Responsive, Recombinant Polypeptide Carriers for Targeted Drug Delivery. Adv. Drug Deliv. Rev. 54, (2002).

[6] Furgeson, D. Y., Dreher, M. R. & Chilkoti, A. Structural optimization of a 'smart' doxorubicin-polypeptide conjugate for thermally targeted delivery to solid tumors. *J. Control. Release.* 110, 362–369 (2006).

[7] Kataoka, K., Harada, A. & Nagasaki, Y. Block Copolymer Micelles for Drug Delivery: Design, Characterization and Biological Significance. *Adv. Drug Deliv. Rev.* 47, (2001).

[8] Varanko, A. K., Su, J. C. & Chilkoti, A. Elastin-Like Polypeptides for Biomedical Applications. *Annu. Rev. Biomed. Eng.* 22, 343-369 (2020).

[9] Li, N. K., Quiroz, F. G., Hall, C. K., Chilkoti, A. & Yingling, Y. G. Molecular description of the lcst behavior of an elastin-like polypeptide. *Biomacromolecules* 15, 3522–3530 (2014).

[10] Despanie, J., Dhandhukia, J. P., Hamm-Alvarez, S. F. & MacKay, J. A. Elastin-like polypeptides: Therapeutic applications for an emerging class of nanomedicines. *J. Control. Release.* 240, 93–108 (2016).

[11] Rizvi, S. A. A. & Saleh, A. M. Applications of nanoparticle systems in drug delivery technology. *Saudi Med. J.* 26, 64–70 (2018).

[12] Chilkoti, A., Christensen, T. & MacKay, J. A. Stimulus responsive elastin biopolymers: applications in medicine and biotechnology. *Curr. Opin. Chem. Biol.* 10, 652–657 (2006).

[13] Macewan, S. R. & Chilkoti, A. Applications of elastin-like polypeptides in drug delivery. *J. Control. Release.* 190, 314–330 (2014).

[14] Meyer, D. E. & Chilkoti, A. Genetically encoded synthesis of protein-based polymers with precisely specified molecular weight and sequence by recursive directional ligation: Examples from the the elastin-like polypeptide system. *Biomacromolecules* 3, 357–367 (2002).

[15] MacEwan, S. R., Hassouneh, W. & Chilkoti, A. Non-chromatographic purification of recombinant elastin-like polypeptides and their fusions with peptides and proteins from Escherichia coli. *J. Vis. Exp.,* (2014).

[16] Dreher, M. R. *et al.* Evaluation of an elastin-like polypeptide-doxorubicin conjugate for cancer therapy. *J. Control. Release.* 91, 31–43 (Elsevier, 2003).